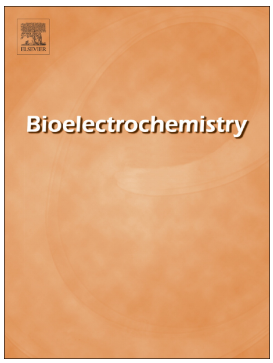

Bioelectrochemical Nitrogen fixation (e-BNF): Electro-stimulation of enriched biofilm communities drives autotrophic nitrogen and carbon fixation

Laura Rago, Sarah Zecchin, Federica Villa, Andrea Goglio, Anna Corsini, Lucia Cavalca, Andrea Schievano

PII: S1567-5394(18)30363-3
DOI: doi:10.1016/j.bioelechem.2018.10.002
Reference: BIOJEC 7211

To appear in: *Bioelectrochemistry*

Received date: 9 August 2018
Revised date: 11 October 2018
Accepted date: 12 October 2018

Please cite this article as: Laura Rago, Sarah Zecchin, Federica Villa, Andrea Goglio, Anna Corsini, Lucia Cavalca, Andrea Schievano , Bioelectrochemical Nitrogen fixation (e-BNF): Electro-stimulation of enriched biofilm communities drives autotrophic nitrogen and carbon fixation. Biojec (2018), doi:10.1016/j.bioelechem.2018.10.002

Bioelectrochemical Nitrogen fixation (*e*-BNF): Electro-stimulation of enriched biofilm communities drives autotrophic nitrogen and carbon fixation

Laura Rago[1], Sarah Zecchin[2], Federica Villa[2], Andrea Goglio[1], Anna Corsini[2], Lucia Cavalca[2], Andrea Schievano[1,*]

[1]*e*-BioCenter – Department of Environmental Science and Policy – Università di Milano, Via Celoria 2, 20133, Milano, Italy

[2]*e*-BioCenter – Department of Food Environmental and Nutritional Science – Università di Milano, Via Mangiagalli 25, 20133, Milano, Italy

[*]Corresponding Author: andrea.schievano@unimi.it

Abstract

A new approach to microbial electrosynthesis is proposed, aimed at producing whole biomass from N_2 and inorganic carbon, by electrostimulation of complex microbial communities. On a carbon-based conductor under constant polarization (-0.7 V *vs* SHE), an electroactive biofilm was enriched with autotrophic nitrogen fixing microorganims and led to biomass synthesis at higher amounts (up to 18 fold), as compared to controls kept at open circuit (OC). After 110 days, the electron transfer had increased by 30-fold, as compared to abiotic conditions. Metagenomics evidenced *Nif* genes associated with autotrophs (both *Archaea* and *Bacteria*) only in polarized biofilms, but not in OC. With this first proof of concept experiment, we propose to call this promising field 'bioelectrochemical nitrogen fixation' (*e*-BNF): a possible way to 'power' biological nitrogen fixation, organic carbon storage and soil fertility against desertification, and possibly a new tool to study the development of early prokaryotic life in extreme environments.

Keywords: biological nitrogen fixation; electro-autotrophy; microbial electrosynthesis; artificial photosynthesis; soil fertility; biocathode; Haber-Bosch process

Introduction

Nitrogen (N) is an essential brick for the synthesis of amino acids, DNA, RNA and proteins: in a single word, for life. Unlike other nutrients (P, K, Mg, etc.) available in the lithosphere, most N on earth is 'locked' in its chemically stable form (dinitrogen, N_2) and accumulated in the atmosphere. During the earth's evolution, N has often been the limiting factor for life in the Biosphere [1]. Biological N fixation (BNF) is the main natural pathway for N to enter biogeochemical cycles [2]. After the Archaean era, BNF was the main source of available N for ecosystems on Earth, with about 203 Tg (10^{12} g) of reactive N produced per year [2]. With the advent of the industrial era, the Haber-Bosch process allowed massive production of ammonia from N_2 (120 TgN yr^{-1}, 80% of which is used as fertilizer in agriculture), relying on massive use of fossil fuels and has been the main route to producing nitrogenous fertilizers. Since then, natural N-cycles have been deeply disrupted by the massive distribution of mineral-N to croplands, with several deleterious imbalances in the biosphere [3]. From a sustainability aspect, N-fertilization should be more territorially distributed, sustainable and based on renewable energy sources. Also, soil enrichment of both carbon and N (as organic matter), instead of free-ammonia, should be pursued, to guarantee the right balance of elements in the pedosphere [4] and long-term soil fertility preservation [5,6].

In nature, the ability to fix atmospheric N_2 is found exclusively among members of the *Bacteria* and *Archaea* domains (called diazotrophs) [7]. Higher living organisms are unable to fix N and eukaryotic photosynthetic organisms (algae, plants) rely on symbiotic interactions with diazotrophs [8].

The biochemistry of BNF is driven by the availability of a) a source of reducing power to allow electron transfer (ET) to a nitrogenase complex and b) a source of chemical energy to store sufficient ATP for the energetic needs of nitrogenase. Heterotrophic diazotrophs harvest both electrons and energy from reduced sugars or carboxylates. This happens in organic-matter-rich environments and in root nodules of leguminous plants [9]. Phototrophic diazotrophs contribute to another consistent share of BNF, harvesting both electrons and ATP from sunlight at sufficient amounts to simultaneously fix N_2 and inorganic carbon [10]. Before photoautotrophic and heterotrophic diazotrophy took over as the two main routes to BNF, lithoautotrophic prokaryotes are known to be the pioneers of BNF, able to harvest electrons and ATP from inorganic reduced molecules, metal ions or minerals (e.g. H_2, H_2S, CO, Fe^{2+}, pyrite), to synthetize organic molecules [11]. Many lithoautotrophs, among pioneer and ancient microorganisms, are also known to be facultative diazotrophs [12–14]. The fixation of inorganic carbon and N_2 by such microorganisms is recognized to be a key pathway to the development of life in extreme environments, such as

protosoils in glaciers or deserts [15,16]. However, they account for a very limited share (<1%) of total N fixed by BNF [2].

Recently, lithoautotrophy has been studied as key mechanism to artificially interact with microbial metabolism by electrical current flow, in the emerging research field of microbial electrochemistry. Microbial electrochemical systems are biotechnological devices that allow the exchange of electrons with microbes and to interfere with their metabolism, by imposing an electrical current. Microbial electrosynthesis (MES), one of the most advanced applications in microbial electrochemistry, is based on this principle: under imposed electrochemical potentials (typically -0.3 – -1 V *vs* standard hydrogen electrode, SHE) [17–19] on solid electrodes (cathodes), autotrophic communities, often forming biofilms, are induced to fix inorganic carbon to produce short-chain carboxylates, alcohols or methane [19–22]. This is based on the capacity of extracellular electron transfer (EET) in certain microbes to use solid materials as electron acceptors or donors to obtain reducing/oxidative power and to conserve ATP for their metabolism [23,24]. When the external material acts as an electron donor, the process has been recently referred to as electro-autotrophy, i.e. a particular type of lithoautotrophy [15,25]. Under such conditions, inorganic carbon is simultaneously the carbon source and the electron acceptor [24]. EET has been described both by direct and indirect paths. Several different mechanisms and membrane proteins involved in EET have been demonstrated in a number of genera of both *Archaea* and *Bacteria* domains [23]. While direct EET was demonstrated to be possible through various membrane bound proteins (e.g. cytochromes) and extracellular electroconductive polymeric substances (recently called nanowires or *e*-pili) [13,26], indirect EET is normally associated with organic (*e.g.* flavins, quinones) or inorganic (*e.g.* H_2, CO, $HCOO^-$) soluble molecules, that act as electron shuttles to microbial whole cells [27]. In many cases, complex biofilms exchange electrons by a combination of these EET mechanisms, allowing lower overpotentials, as compared with 100% abiotic electrocatalysis towards similar reactions [21,28,29].

In this work, we propose to merge microbial electrosynthesis and BNF. We hypothesize that electro-autotrophic metabolism would be a possible path to simultaneously fix inorganic carbon and N_2, i.e. to drive the synthesis of new microbial biomass from air, water and electricity. Solid electrodes could serve as electron donors for both inorganic carbon and N fixation, by enriched autotrophic biofilm communities.

Previous experiments had conceived artificial BNF at room temperature to obtain free ammonia, by using enzymatic catalysis, i.e. based on incorporating nitrogenase enzymes (obtained from the diazotroph *Azotobacter Vinelandii*) on polarized electrodes [30]. Others have tried a similar 'enzymatic' approach. Paschkewitz et al. [31,32] attempted an 'electro-enzymatic' approach by

coating a glassy carbon electrode with a mix of a polymer (Nafion and dried cells of *A. variabilis*, cultivated in N-starvation conditions). They observed ET, mediated by Fd- and NADH, from the electrode to the enzymatic pool (nitrogenase and nitrate/nitrite reductase) of *A. variabilis*, driving ammonia formation.

These approaches encouraged the combination of BNF with MES: when electrons are successfully shuttled from a polarized electrode to intracellular redox mediators such as NADH and Fd, the enzymatic system of diazotrophs can evolve significant amounts of ammonia from N_2. However, the 'enzymatic' path might limit the durability and applicability of such systems. Also, by such an approach, inorganic carbon is not fixed and N remains in the form of free ammonia.

More recently, Liu and colleagues demonstrated the possibility of using living cells coupled to an electrochemical system, towards N fixation [33]. They generated H_2 by electrochemical water splitting using a specific abiotic catalyst (Co-P alloy) and imposing a cathodic polarization of around -0.7 V *vs* SHE, pH 7. This H_2 diffused through the bulk growth medium of a planktonic pure culture of *Xanthobacter autotrophicus* (a known lithoautotroph), as source of reducing power for simultaneous C and N fixation. The main limits of this experiment, towards possible future applications to real-life, were: a) the difficult applicability of pure cultures to real scales due to sterility issues; b) the inefficiency of producing soluble-H_2 in a bulk liquid and to make it available to planktonic microbial cells; c) the use of a relatively expensive and technological inorganic catalyst, such as Co-P for H_2 evolution; d) the relatively high potential difference applied to the system (ΔE = 3 V), needed to overcome abiotic reaction overpotentials.

Herein, we present the first study where a mixed microbial community was enriched directly on a plain carbon-fiber electrode (no abiotic catalyst), as a complex biofilm. As typically happens in MES, electro-active complex communities can be enriched on an electrodes surface and form a biofilm, which completely changes the electrochemical overpotentials of electrode reactions, because a combination of abiotic and biotic reactions influence the EET [19,34]. Also, interactions between different metabolic pathways might help in sustaining overall biomass production, as compared to the pure-culture approach.

Materials and methods

Double-chambered bioelectrochemical reactors were run in parallel for 110 days, under autotrophic and N-starvation conditions, at 25 °C, in complete darkness. Plain carbon-cloth electrodes, without any specific abiotic catalyst, were continuously polarized by Nanoelectra Nev 4 potentiostats (Spain), at -0.9 V *vs* Ag/AgCl (sat. KCl) reference electrodes (nearly -0.7 V *vs* SHE). This potential was chosen after electrochemical measurements on the experimental set-up, to avoid abundant H_2 evolution by abiotic reactions. Due to the relatively high overpotentials generated by this

experimental configuration, typical H_2-evolution currents were observed below -0.8 V vs SHE in linear sweep voltammetries (**Figure S0**, supplementary materials).

One reactor was under air-exposed (AE) conditions, while another under strict anaerobic (AN) conditions (N_2 atmosphere). Two other identical reactors were set up under the same oxygen-exposure conditions and served as control at open circuit (OC). All cathodic chambers were inoculated with a mixed microbial consortium, obtained from different environmental sources. To favor a biofilm-forming cathodic community over planktonic cells and to restore N-starvation and autotrophic conditions, the bulk medium in all reactors was completely replaced with an N- and organic-C-deficient medium at days: 15, 28, 37 and 78.

Bioelectrochemical reactors and electrochemical measurements

The bioelectrochemical reactors were made with pairs of 125-mL bottles, connected by a lateral neck. A proton exchange membrane (Nafion 117) separated the anodic and cathodic chambers. Cathodes were made of plain carbon cloth (geometric area: 250 cm^2), rolled-up cylindrically, while counter electrodes were made of stainless steel grid, with an identical geometric area.

The systems were tested under abiotic conditions by linear sweep voltammetry and chronoamperometry for around 15 days. This was repeated after inoculation (day 1) and several times during the experiment, to follow biofilm growth. Sweep voltammetry (between -0.4 to -0.7 V *vs* SHE) was performed only on polarized reactors (AE and AN), to determine the intensity generated at different points in the experiment. Neither chronoamperometric nor polarization tests were applied on OC reactors (AE-OC and AN-OC), to avoid possible electrostimulation of the OC biofilms.

Culture medium

Both chambers of each reactor were filled with 100 ml of a culture mineral medium [35], modified by omitting bioavailable N sources. Each liter contained 10 g of K_2HPO_4 and 10 ml of trace element solution. The trace element solution (1 liter) was prepared with 0.5 g Na_2-EDTA, 0.2 g $FESO_4 \cdot 7 H_2O$, 0.1 g $ZnSO_4 \cdot 7 H_2O$, 0.03 g $MnCl_2 \cdot 4 H_2O$, 0.3 g of H_3BO_3, 0.2 g $CoCl_2 \cdot 6 H_2O$, 0.01 g $CuCl_2 \cdot 2 H_2O$, 0.02 g $NiCl_2 \cdot 6 H_2O$,0.03 g $Na_2MoO_4 \cdot 2 H_2O$. Each solution was prepared using ultra-pure water (milliQ®, Merck). The medium was autoclaved before the addition of 10 g of $NaHCO_3$. The bicarbonate buffer ensured the source of CO_2 and pH stability around 8. Before each medium replacement in the bioelectrochemical reactors, the medium was sparged with pure N_2 gas and pH was adjusted to 8.0.

Inoculum and system start-up

The cathodic chamber was inoculated with a mixed microbial community harvested from: a) the anaerobic sludge (2 mL for each reactor) from the anaerobic digester of a municipal wastewater

treatment plant (Milan, Italy) and b) filtered (1 mm mesh) bovine manure (1 mL) from a farm near Milan. The start-up period lasted 10 days, during which the medium was replaced twice. The first time the medium was replaced with 50% of fresh medium and 50% of reactor broth of the previous batch cycle. In the second cycle, the medium was totally replaced with the organic N and C free fresh medium, to maintain both C- and N-starvation conditions.

After the start-up period, the experiments were run for over 110 days, with the culture medium changed five times in the cathodic chamber, after increasing incubation periods (from 15 to 30 days), to favor the biofilm community over planktonic cells and to periodically restore N-starvation conditions.

Total Organic Carbon (TOC) and Total Kjeldahl Nitrogen (TKN)

Total Organic Carbon (TOC) was analysed using a SIEVERS 820 Portable Total Organic Carbon Analyzer (GE Analytical Instruments, UK). This tool provides an extremely sensitive measurement of the TOC concentration in water solutions [36], by measuring conductivity in a deionized water solution, where the CO_2 coming from TOC mineralization is dissolved. Inorganic carbon in the sample is measured in a parallel channel, where mineralization is not performed. Before the injection, 1 mL of sample was treated for 30 minutes in a solution of 1 mL of phosphoric acid and 23 mL of deionized water to decrease inorganic carbon concentration and avoid interference. Then, 1 mL of solution was injected into the analyser. This procedure was repeated three times (triplicate). TKN was determined in triplicate by ammonium distillation and titration (with H_2SO_4), after digestion of nearly 50 mL of bulk sample in H_2SO_4.

Total planktonic cell count

50 ml of bulk samples were fixed, stained with DAPI (4',6-diamidino-2-phenylindole) and observed with a fluorescence microscope. DAPI analyses were performed on the planktonic community at the end of each cycle. Cells in 100 mL medium were fixed by adding 1.0 mL of 4% paraformaldehyde and stored for 3 h at 4°C. Following fixation, the samples were centrifuged at 10000 rpm and the pellets obtained were rinsed using PBS and stored in 50% ethanol, 50% PBS at −20 °C. Each pellet was stained using DAPI following the protocol described by Zecchin et al. [37]. The samples, after dilution in NaCl solution (9 g L^{-1}), were mixed with DAPI solution to a final concentration of 5 µg mL^{-1} and incubated at room temperature for 15 min in the dark. Samples were then immobilized on black 0.2 µm Isopore™ GTBP membrane filters (Millipore). After drying, the filters were mounted on glass slides with Vectashield mounting medium (Vector Laboratories, Burlingame, CA, US), in order to reduce autofluorescence of the samples, and observed with a fluorescence microscope (Zeiss Axioskop) supplied with a Mercury Short Arc HBO 50W/ACL2 OSRAM UV lamp and Zeiss 1 filter sets for DAPI. The cells were counted in 20 microscopic fields using a calibrated grid.

Measurements of soluble molecules in the bulk liquid phase

NH_4^+, NO_3^- and NO_2^- were measured after filtration (0.2 μm nylon filters) using HACH vials and HACH DR220 Vis-spectrophotometer, following the standard procedure for each analyte. Detection limits of concentrations, for NH_4^+, NO_3^- and NO_2^-, were 0.01 mgN L^{-1}. Low molecular weight organic fatty acids (acetic, propionic, iso-butyric, butyric, valeric) were determined using a gas-chromatograph Varian CP-3800 equipped with FID detector and a gas capillary column NUKOL, 30 m x 25 mm, diameter: 0.25 mm, by SUPELCO. FID was run at 250 °C. Detection limits of such procedure were 0.1 mg L^{-1}.

Headspace gas analysis

O_2, H_2, CH_4, CO_2 and N_2 concentrations were sporadically measured in the headspace through gas chromatography, using thermal conductivity detectors (Micro GC 3000, Agilent Technology, Santa Clara, CA, USA) [38].

Cathodic biofilm imaging by Confocal Laser Scanning Microscopy (CLSM)

The structure and the architecture of biofilms growing on cathode surfaces of the four reactors after 37 and 110 days of operation were investigated by CLSM as previously reported by Villa et al. [39,40].

A lectin Concanavalin A-Texas Red conjugate (ConA, Invitrogen, Italy) was used to visualize the polysaccharide component of biofilm matrix (extracellular polymeric substances, EPS), whereas Syto 9 green fluorescent nucleic acid stain (Invitrogen, Italy) was used to display biofilm cells. Cathode samples were incubated with 200 μg μl^{-1} ConA and 5 mM Sito-9 dye solution in ddH_2O at room temperature in the dark for 30 min, and then rinsed. Confocal images were collected using a Leica TCS-SP5 confocal microscope (Leica Microsystems Heidelberg GmbH, Germany) and a 40X 0.7NA water immersion objective or a 1X dry lens objective. Fluorescence was excited and detected using the following laser lines and emission parameters: for Syto 9-stained cells, ex 488 nm laser, em 500 to 550 nm, and for ConA-stained EPS ex 561 nm laser, em 570 to 620 nm. In addition, the CLSM was used in reflectance mode with the 488 nm argon line for relief imaging of carbon fiber cloths. Captured images were analyzed with Imaris software (Bitplane Scientific Software, Switzerland) for 3D reconstruction. At least six biofilm images were collected for each sample and representative images were selected.

Total DNA extraction from cathodic biofilms

After the enrichment period (day 37) and at the end of the experiment (day 110), nucleic acids were extracted from cathodic carbon cloth samples obtained from the four reactors. Total DNA was extracted from approximately 0.25 g of samples, using a PowerSoil DNA Isolation Kit (MoBio Laboratories, Inc., Carlsbad, CA,USA) according to the manufacturer's instructions. The quantity

and the quality of extracted nucleic acids were measured by spectrophotometry (BioPhotometer, Eppendorf) and visualized under UV light in a 1% gel electrophoresis with TAE × 0.5.

Whole genome shotgun sequencing and bioinformatic analysis

Shotgun metagenomic libraries were prepared using a Illumina Nextera DNA library preparation kit (Illumina, Inc., USA) with total DNA input of 40–50 ng, as per manufacturer's instructions. The resulting DNA fragment libraries were cleaned up with Agencourt AMPure XP beads (Beckman Coulter, Inc., USA) and fragment size within the range of 300–700 bp was verified by running in a 2100 Bioanalyzer using an Agilent High Sensitivity DNA chip. Multiplexed DNA libraries were quantified with KAPA Library Quantification Kit and normalized to 2nM following standard protocols for sequencing in the Illumina MiSeq platform. Finally, pair-end sequencing was performed with a MiSeq V2 chemistry (150x2) through the Illumina MiSeq platform.

Output fastq files were assembled with Spades 3.7 [41] using standard settings. Assemblies were uploaded on the MG-RAST server (MetaGenome Rapid Annotation using Subsystems Technology [42]) for automatic annotation.

From the metagenomics libraries, sequences classified as subunits of the nitrogenase complex after comparison with the COG database (Clusters of Orthologous Groups of proteins [43]) were extracted and individually compared with the NCBI database using BLASTP [44]. Similarly, sequences of genes related to ET as cytochromes C, type IV pili and ET flavoproteins (COG2025) were extracted from the metagenome. Molecular phylogenetic analysis of the sequences encoding one of the nitrogenase complex subunit was inferred with the Maximum Likelihood method using MEGA [45].

Fluorescent in situ hybridization (FISH) analyses of cathodic biofilms

Fluorescence in Situ Hybridization (FISH) was performed on carbon cloth pieces obtained from the cathode surfaces of the four reactors after 37 and 110 days of operation. Carbon cloth samples were cut from the cathodes and carefully transferred into sterile tubes (2 mL capacity) to minimize disruption of the biofilms. Cells were fixed by adding 1.0 mL of 4% paraformaldehyde and stored for 3 h at 4°C. After fixation, the samples were gently rinsed using PBS and stored in 50% ethanol, 50% PBS at −20°C.

Sections of carbon cloths were hybridized with 5′-, 3′-doubly labeled probes EUB338 (doubly labeled with Cy5, specific for the domain Bacteria) and ARCH915 (doubly labeled with Cy3, specific for most Archaea). Double-labeled probes were obtained from Thermo Hybaid (Interactiva Division, Ulm, Germany) and used to increase the probe signals, overcoming possible low cellular ribosome content[46].

FISH was performed as previously described by Cappitelli et al. [47] with the following modifications. Briefly, carbon cloth samples were rapidly immersed in a pre-warmed hybridization buffer (0.9 M NaCl, 20 mM Tris–HCl pH 7.2, 0.01 % wt/v SDS, 30 % v/v deionized formamide, 1 ng/µl of each probe) and incubated overnight at 46 °C. After hybridizations, the samples were washed for 20 minutes at 48 °C in a washing buffer to remove the unbound probes. Finally, the samples were rinsed with cold distilled water and air dried.

The specificity of the rRNA hybridization, was checked by treating permeabilized samples with an RNase cocktail as reported by Villa et al.[48]. Hybridized carbon cloth sections were inspected by CLSM as previously reported. Captured images were analyzed with the Imaris software (Bitplane Scientific Software, Switzerland) for 3D reconstruction. MetaMorph Imaging software (Molecular Devices, Sunnyvale, CA, USA) provided quantitative data of biovolumes occupied by the two different fluorescent probes. Using region tools, both the green (Bacteria) and red (Archaea) areas for all planes of a stack were measured and then multiplied by the Z-axis distance to calculate the corresponding biovolumes. A minimum of seven biofilm images were analyzed for each sample and representative images selected.

Adjustment of the brightness/contrast and level settings was applied to the entire images. Processing of individual images was identical to ensure comparison between samples.

Quantitative real-time PCR

The 16S rRNA genes of *Bacteria* and of *Archaea* were evaluated for the quantification of the microbial community in cathodic carbon cloth samples. Primers for quantification of Bacteria 16S rRNA genes were Eub338F (5'-ACT CCT ACG GGA GGC AGC AG-3') and Eub518R (5'-ATT ACC GCG GCT GCT GG-3'), they were used at final concentration of 200 nM in a reaction performed according to the literature [49].

Primers for the quantification of Archaea 16S rRNA genes were ARC787F (5'-ATTAGATACCCSBGTAGTCC-3') and ARC1059R (5'-GCCATGCACCWCCTCT-3'), they were used at a final concentration of 500 nM according to Yu et al. [50]. All the reactions were set up in a 20 µL mixture volume containing 1x Titan HotTaq EvaGreen® qPCR Mix (Bioatlas), primers at above-mentioned concentrations, 2 µL of template DNA and PCR-grade water (Sigma-Aldrich). When necessary, appropriate dilutions of DNA were made to fit Cq values of samples into standard curves. Real Time qPCR reaction was performed on a MJ Mini™ cycler equipped with a MiniOpticon™ system (BIO-RAD, USA). The melting curves were calculated at the end of each run. Each sample was amplified in triplicate and no-DNA controls were run in parallel. To calculate the gene copy number, standard curves were created by amplifying known amounts of DNA isolated from cloned plasmids containing the targets [37,51].

Illumina MiSeq 16S sequencing

Genomic DNA was PCR-amplified using a two-stage "targeted amplicon sequencing (TAS)" protocol [52,53]. The sequencing procedure was performed as described previously [54]. The primers contained 5' common sequence tags (known as common sequence 1 and 2, CS1 and CS2) as described previously [55]. Two primer sets were used for this study, including CS1_341F/CS2_806R (*Bacteria*), CS1_ARC344F/CS2_ARC806R (*Archaea*) [54].

Library preparation and pooling was performed at the DNA Services (DNAS) facility, Research Resources Center (RRC), University of Illinois at Chicago (UIC). Sequencing was performed at the W.M. Keck Center for Comparative and Functional Genomics at the University of Illinois at Urbana-Champaign (UIUC).

Forward and reverse reads were merged using PEAR [56]. Ambiguous nucleotides and primer sequences were trimmed (quality threshold $p = 0.01$). After trimming, reads containing internal ambiguous nucleotides, lacking either primer and/or shorter than 300 bp were discarded. Chimeric sequences were identified with the USEARCH algorithm [57] and removed. Further analyses were performed with the QIIME tools [58]. Sequences with a similarity higher than 97% were grouped in Operational Taxonomic Units (OTUs) and representative sequences for each OTU were aligned to the SILVA SSU Ref dataset [59] using the PyNAST method [60]. After taxonomic assignment, OTU tables were generated for each sample.

Results and discussion

As confirmed by abiotic experiments (**Figure S0** of **Supplementary materials**), consistent H_2 evolution (observed as increased slope of polarization curves) started below cathodic potentials of around E = -0.8 V *vs* SHE (**Figure 1a,b**). Under abiotic conditions, cathodic currents at E = -0.7 V *vs* SHE were only around 0.08 mA (**Figure 1a,b**). This corresponds to around 150 times less than currents generated in the experiment by Liu et al., at the same cathodic potential (-0.7 vs SHE) and with similar electrode areas and reactors geometry, while in the presence of the specific abiotic catalyst of hydrogen evolution reaction (Co-P alloy) [33]. In our experiment, where no specific catalyst was present on the carbon cloth surface, H_2 evolution by abiotic water splitting likely had a marginal role in ET at E = -0.7 *vs* SHE. Only at lower cathodic potentials (E < -0.8 V *vs* SHE), polarization curves showed incremental slopes, typical of H_2 evolution (**Figure 1a,b**). As further confirmation of this hypothesis, H_2 was never detected in any reactor headspaces. Only trace concentrations of methane were detected in the headspace of AN, while CH_4 concentrations were below the detection limit in all other reactors (**Table S1**).

After inoculation, a consistent increase of polarization current intensity at E = -0.7 V *vs* SHE, observed during the experiment, compared with day 1 (**Figure 1a,b**). This suggests that electroactive microbial communities were progressively establishing on cathodes, consistently boosting the ET, as compared to the abiotic conditions. While abiotic ET was marginal, polarization currents at E = -0.7 V *vs* SHE increased to around 1 mA for both AE and AN, along with biofilm establishment on cathodes (e.g. days 37 and 56). At day 110, cathodic polarization currents in AE reached almost 4 mA (50-fold increase as compared to day 1, **Figure 1b**). Such an increase in ET (1-2 orders of magnitudes) was possibly linked to several biotic interactions with the surface of the carbon cloth, including direct EET to the microbial biofilm. In support of this hypothesis, metagenomics analysis applied to cathodic biofilm DNA (**Table 1**), sampled at day 37, evidenced the presence of several genes encoding well-known proteins [18,29,34,61,62] associated with direct (different categories of cytochromes-C and type IV pili) or indirect (flavoproteins COG2025) EET (**Table 1**). ET flavoproteins (COG2025), different categories of cytochromes-C and type IV pili were retrieved in all samples (**Table 1**). Up to twice the number of such genes were retrieved in polarized trials, as compared to OC controls (**Table 1**).

Table 1 - Summary of the output of Illumina shotgun sequencing performed on samples obtained from the cathodic biofilms after the enrichment period (day 37).

Sample	Raw Reads	Contigs	Av. Length (bp)	16S rRNA gene sequences	Nitrogenase subunit sequences	ET genes
AN-OC	1023878	78661	310	116	9	110
AN	1541178	116383	383	130	12	158
AE-OC	513010	44360	341	57	0	50
AE	1050650	91466	304	112	16	121

At day 110, AE showed 3-times higher cathodic currents as compared to AN (**Figure 1 a,b**). This resulted in a higher amount of cumulative charge transfer along the 110 days (423 C *vs* 265 C) (**Figure 1c,d**). Microscopic investigations of representative portions of cathodic biofilms revealed the evolution (along 110 days) of consistent structures in AE, as compared to all other trials (**Figure 2**). At day 110, the colonization pattern of AE samples visibly increased (in comparison to day 37, **Figure S1**), showing a network-like structured biofilm spreading among the carbon cloth fibers and occupying the whole surface (**Figure 2**).

The biofilm spatial patterns which emerged at day 110 in AN, as well as in OC controls (both AN-OC and AE-OC) were different. As compared to day 37 (**Figure S1**), the biofilm in AN at day 110

appeared to decrease in biomass volume and showed deterioration (**Figure 2**). Similar dramatic reduction of biofilm cluster size and loose assemblages of cells were observed in OCs, suggesting the impairment of the biofilm integrity (**Figure 2 and Figure S1**). Interestingly, the impairment of biofilm in AN observed at day 110 (**Figure 2**) was perfect in accordance with the slight decrease in cathodic polarization currents shown in **Figure 1a** after day 37. This further confirms that the ET processes were substantially mediated by biotic electro-activity.

Representative FISH images of the cathodic biofilms (**Figure 2** and **Figure S2**) confirmed that, in AE cathodic biofilms, the proportion of both bacterial and archaeal ribosomes significantly increased over time (day 110 *vs* day 37) in comparison with all other biofilm samples. Three-dimensional reconstruction of the AE biofilm revealed an inner core region where a cluster of microorganisms of the *Archaea* domain were located and covered by a thick layer of *Bacteria* (**Figure 2**). Possibly, ET favored local anaerobic conditions on the cathode surface, despite the air-exposure.

Quantitative and semi-quantitative analyses confirmed this scenario. Biovolumes of both archaeal and bacterial communities (**Figure 3**) significantly increased over time in AE (see values of day 37 in **Figure S3**), as compared with the control AE-OC (for both *Archaea* and *Bacteria*). Quantitative real-time PCR (qPCR) confirmed this result: AE showed the highest amount of *Archaea* 16S rRNA gene copies at day 37 (**Figure S3**) and this number increased by 4-fold at day 110 (**Figure 3**), while strongly decreasing in AE-OC. *Bacteria* also increased exclusively in AE (**Figure 3 and Figure S3**), while decreasing in AE-OC biofilms. By contrast, the 16S rRNA gene copies for *Archaea* were not significantly different in AN and AN-OC and did not significantly vary with time (day 37, **Figure S3** and day 110, **Figure 3**). Accordingly, *Archaea* and *Bacteria* biovolumes tended to decrease or remained constant.

Figure 3 also shows quantitative measurements of biomass suspended in the bulk medium (as TOC, TKN and cells). Mineral forms of N (NH_4^+, NO_2^-, NO_3^-) as well as soluble organic C-sources (volatile fatty acids C2-C6), were found to be below detection limits (0.01 mg L^{-1}) along the experiment. Therefore, heterotrophic microbial growth in the bulk liquid phase was likely limited. In parallel, autotrophic metabolism supported by H_2 diffusion to the bulk phase was likely negligible, as observed from polarization curves (**Figure 1**). These observations lead us to hypothesize that biomass was released into the liquid phase mainly from biofilms.

The average rates of biomass release (days 37 - 110) was 3- to 6-fold higher in the presence of current flow, as compared to OCs, in both AE and AN. In the case of AE, this increase mirrored that observed for biofilms (**Figure 3**). In AN, the final part of the experiment indicated that biofilm structure was compromised. Despite that, quantitative determinations of microbial biomass released

into the bulk medium were significantly higher than in AN-OC (**Figure 3**). These findings support the effect of electrostimulation on biomass synthesis under polarization, as compared to OC conditions.

We assume that these differences represent the C and N fixed by autotrophic/diazotrophic metabolism and, in parallel, possible additional N fixed by heterotrophic diazotrophs. In this hypothesis, the rates of biomass synthetized and released into the bulk liquid would result in around 0.3 mgC L^{-1} d^{-1}, 0.2 mgN L^{-1} d^{-1} or $5^{*}10^{9}$ cells L^{-1} d^{-1}. Unfortunately, a complete quantitative balance of C and N to also account for the biofilm, could not be performed in this experiment. However, the remarkable increase in biomass, observed in both biofilm (for AE) and bulk liquid as compared to OC controls (**Figure 3**), suggests that electrostimulation of electro-autotrophic routes towards N- and C-fixation must have represented the key-factor for biomass synthesis. We propose to call this process bioelectrochemical N fixation (*e*-BNF). **Figure 4** shows the concept of *e*-BNF and hypothesizes the future use of such process for engineered applications aimed at restoring/improving soil fertility, against desertification.

Metagenomics applied on cathodic biofilms DNA (**Figure 5, Table 1**) strongly supports these assumptions: metagenomes evidenced the presence of *Nif* genes associated with autotrophic metabolism only in polarized trials (AE, AN), but never in controls (AE-OC, AN-OC).

Table 1 shows a summary of the output of Illumina shotgun sequencing. On average, 1 Mio reads were obtained for each sample, resulting in the assembly of 90000-100000 contigs with average length 340 bp. From sample AE-OC, a lower amount of raw reads and subsequent assembled contigs were retrieved, as compared to the others. Sequences encoding different nitrogenase complex subunits *NifDEKNHQ* were retrieved in AE and AN, and in AN-OC, whereas nitrogenase-related sequences were absent in AE-OC (see **Table 1**). Sequences for subunits *NifDEKN* were found in both AE and AN, while *NifH* only in AE. *NifN* and *NifQ* were found in AN-OC.

Phylogenetic analysis (**Figure 5**) allowed accounting for a wide variety of bacterial as well as archaeal species potentially involved in the expression of N-fixation. *Nif* sequences belonging to *Methanobrevibacter arboriphilus* were retrieved only in polarized reactors (AE and AN) biofilm samples. *Nif* sequences related to *Candidatus Accumulibacter spp.* were present only in AE and AN. Other *Nif* sequences belonging to *Shewanella mangrovi* and to *Methylomonas koyamae* were retrieved in the AE cathodic biofilm. In summary, the cathodic biofilms were colonized by autotrophic N_2-fixers exclusively under polarization conditions (AE and AN) (**Figure 5, Table 1**). In fact, no genes encoding nitrogenase were found in AE-OC (**Table 1**). In AN-OC, no nitrogenase gene could be associated with autotrophic metabolism (**Figure 5, Table 1**): heterotrophs represented the totality of N_2-fixing guild in AN-OC system (all the 9 subunit sequences reported in

Table 1). All *Nif* sequences retrieved in OC controls (only in AN-OC) belonged to facultative aerobic heterotrophs close to *Azonexus hydrophilus* and *Azoarcus* sp.. These were potential contributors to heterotrophic N-fixation, where residual available organic carbon was present in the biofilm environment. It is likely that anaerobic conditions preserved residual organic carbon to sustain heterotrophic diazotrophs, while more oxidative conditions in AE-OC, helped in depleting such organic C-sources.

Organic molecules derived from biodegradation of residual biofilm and dead microbial cells could have served as possible electron donors for heterotrophic microbial growth, regardless of the polarization imposed. Indeed, many genera and *Nif* genes found in AE, AN and AN-OC biofilm samples (**Figure 5, Figure 6**), were associated with heterotrophic metabolism. In the presence of bioavailable forms of organic carbon, several heterotrophs could fix N and sustain their growth, also in the absence of polarization. This is true, for example, for *Azoarcus* sp. and *Azonexus hydrophilus* found in AN-OC, AN and AE. These bacteria were found to possess nitrogenase genes (**Figure 5**), as confirmed in the literature [63,64]. Additionally, *Thauera sp.* (**Figure 6**) is known to perform either heterotrophic anaerobic respiration of nitrate or selenite and chemolitho-autotrophy using hydrogen and carbon dioxide [65,66].

In addition, several methanotrophic N-fixers (e.g. *Methylomonas koyamae, Methylogaea oryza, Methylocaldum szegendiense*) were retrieved solely under electro-stimulation, in both AE and AN (**Figure 5 and 6**). According to other studies, these species are able to use methane or methanol as carbon and energy source [67], while fixing N_2 [68]. These methanotrophic diazotrophs probably short-circuited the methane produced by the underlying layer of *Archaea* (**Figure 2**), to grow and fix N. Indeed, CH_4 was detected only in AN at trace concentrations (**Table S1**). A direct interspecies ET (DIET) in synthrophic association could also be possible, without intermediate methane production [69].

The most relevant autotrophic diazotroph was the strict anaerobe *Methanobrevibacter arboriphilus*. *Nif* genes associated with this species were found in the metagenome of AE and AN (**Figure 5, Figure 6**). *M. arboriphilus*, previously described as an hydrogenotrophic methanogen [70], was found in several biocathodes of microbial electrolysis cells and electro-methanogenic reactors [51,71,72]. *Methanobrevibacter* species were often associated also with DIET, in syntrophic partnership with other electroactive bacteria, as recently reviewed [73]. Interestingly, AE biofilm contained *nifD* genes belonging to *Shewanella* sp. and *Pelobacter* sp. (**Figure 5**), which are widely recognized to possess conductive pili and membrane cytochromes for DIET [74]. The presence in AE of these electroactive microorganisms might have empowered both ET and C/N fixation in the biofilm community. In the complex microbial community established as cathodic biofilms, other

autotrophic N-fixers [75–77] might have played a role in biomass synthesis. *Nif* genes of *Candidatus Accumulibacter sp.*, *Sideroxydans sp.*, *Ferriphaselus amnicola* were retrieved in both AE and AN (**Figure 5, Figure 6**). Electro-autotrophic activity likely stimulated N-fixation of these known lithoautotrophic diazotrophs.

Starting from these observations, three possible paths driving *e*-BNF were likely to occur in the cathodic biofilm, towards the synthesis of biomass (**Figure 7**):

1) single microbial strains with simultaneous diazotrophic and electro-autotropic metabolic abilities yield sufficient reducing equivalents from EET and ATP for both CO_2 and N_2 fixation. This was the case for some *Archaea* (forming an inner layer at cathode interface, covered by *Bacteria*, **Figure 2**) or electroactive autotrophs with diazotrophic capabilities;

2) electro-autotrophic and diazotrophic metabolisms could mutually work by syntrophic associations among different species. Available organic-C forms deriving from biofilm and CH_4 produced by *Archaea* could sustain heterotrophic or methanotrophic diazotrophs, which in turn could fix sufficient N in bioavailable forms, as to sustain electro-autotrophs.

3) syntrophic association among electro-autotrophs and other N-fixers (e.g. between *Methanobrevibacter* and *Shewanella/Pelobacter*) by DIET is an option.

Certainly, real proof of such hypothesized mechanisms (see further discussions on **Supplementary materials**) needs to be confirmed in further experiments, by performing meta-transcriptomic analysis on both biofilms and bulk liquid microbial communities.

Conclusions

Here, an explorative experiment was performed to 'open' this new field. We demonstrated that it is possible to induce simultaneous BNF and inorganic carbon fixation by imposing electrical stimulation to a mixed microbial community, as a unique source of reducing power. From such preliminary observations, we propose to open a brand new branch of fundamental research in the field of microbial electrochemistry: *e*-BNF, as a step beyond MES, would allow the synthesis of whole biomass, instead of single organic molecules. The possibility to electrically stimulate biomass synthesis, through simultaneous C- and N-fixation, might open a new path towards sustainable and local on-demand N-fertilizer production, based on renewable power. In the future, *e*-BNF might find engineered applications to enhance soil organic matter storage and to preserve soil fertility against desertification. In parallel, new scientific options could be opened in the study of early microbial life on Earth and in extreme environments. *e*-BNF might become a useful tool to understand the mechanisms of electron shuttling in soil niches more deeply, towards energy conservation and N-fixation. Finally, lithoautotrophic N-fixation is also one of the key-mechanisms

in biocorrosion. Controlling *e*-BNF mechanisms might prove to be fundamental as biocide technique to avoid biocorrosion in industrial facilities or historical monuments.

A repeat of these findings and deeper insights are needed to support these observations and the hypotheses made in this article. Future experiments should aim at striking a quantitative balance of biomass (e.g. using isotope-labelled C and N), at studying the metatranscriptome or metaproteome, to understand the active biochemical mechanisms involved, and at increasing C- and N-fixation rates.

Acknowledgments

This work has been entirely financed by the Italian Ministry of University and Research (MIUR), within the SIR2014 Grant, project RBSI14JKU3. Part of the work was also made possible by microscope facilities at the Center for Biofilm Engineering at Montana State University, which were supported by funding obtained from the NSF-MRI Program and the M.J. Murdock Charitable Trust. Authors also acknowledge Dr. Stefania Marzorati, Dr. Stefano P. Trasatti (Department of Environmental Science and Policy), Dr. Matteo Compagnoni and Prof. Ilenia Rossetti (Department of Chemistry) of the University of Milan, for their contribution to electrochemical lab and headspace gas analyses.

Figure 1 – Cathodic polarization current intensity during linear sweep voltammetry performed along the experiment under anaerobic (**a**) and air-exposed (**b**) conditions; dashed lines correspond to the potential of E = -0.7 *vs* SHE, utilized for chronoamperometry along the experiment. Trends of current densities measured on cathodic surface by chronoamperometry under anaerobic (**c**) and air-exposed (**d**) conditions, along a representative period (days 80-90).

Figure 2 - (**a,b**) Confocal laser scanning imaging and FISH-CLSM analysis of cathodic biofilms at day 110, under anaerobic (**a**) and air-exposed condition (**b**). The images correspond to three-dimensional blend reconstructions obtained from confocal images series with the dedicated IMARIS software, including virtual shadow projections on the right-hand side to represent biofilm sections. Color key: Biofilm cells, green (Syto9); EPS matrix, red (ConA); cathodic surface, grey (reflection). (**c,d**) FISH-CLSM analysis reveals bacterial (first line) and archaeal (second line) communities, under anaerobic (**c**) and air-exposed condition (**d**). Color key: *Eubacteria*, green (probe EUB338); *Archaea*, red (probe ARCH915); cathodic surface, grey (reflection). Scale bars represent 20 or 30 µm. Larger images report polarized trials, while smaller the corresponding open circuit control.

Figure 3 - Biomass abundance at day 110 in the biofilm (**a, b**) and released to the bulk liquid (**c**), under polarization (dark grey) and in open circuit controls (light grey). Cathodic biofilm biomass of both bacterial (**a**) and archaeal (**b**) communities was evaluated by semi-quantitative biovolumes estimation associated to FISH-CLSM analysis and quantitative determination of 16S rRNA gene copies by qPCR. Average (days 37-78) rates of biomass release to the bulk liquid phase (per liter of reactor volume per day), as total organic carbon (TOC), total Kjeldahl nitrogen (TKN) and suspended microbial cells count (with DAPI dye) (**c**).

Figure 4 – The concept of bioelectrochemical nitrogen fixation (*e*-BNF) and its potential application to enhance soil fertility. The average rates of electro-stimulated biomass synthesis measured in this experiment (days 37 - 110) are reported, net of controls.

Figure 5 - Nitrogenase genes retrieved in cathodic biofilms by metagenomics (by Illumina Nextera DNA library). Maximum Likelihood trees constructed with sequences affiliated to NifDE (**a**), NifNK (**b**), Nif(H) (**c**) and NifQ (**d**) obtained from samples (AE, AN, AE-OC and AN-OC). The outgroup of NifQ tree is represented by the NifDE tree. Evolutionary analyses were conducted in MEGA6 [45]. The evolutionary history was inferred by using the Maximum Likelihood method based on the Tamura-Nei model [45]. The trees with the highest log likelihood (-23594.0678, -3896.7308 and -20091.6604 for **a**, **b** and **c** respectively) are shown. Initial tree(s) for the heuristic

search were obtained by applying the Neighbor-Joining method to a matrix of pairwise distances estimated using the Maximum Composite Likelihood (MCL) approach. The trees are drawn to scale, with branch lengths measured in the number of substitutions per site. The analysis involved 75, 20 and 51 amino acid sequences, respectively, with a total of 647, 341 and 670 positions in the final dataset.

Figure 6 - Microbial diversity of cathodic biofilms at the end of the experiment (day 110). Genus representation of Illumina 16S rRNA gene amplicon sequencing.

Figure 7 – Proposed schematic representation of potential mechanisms driving *e*-BNF in a mixed microbial community, according to the genetic pool observed in this study. *e*-BNF is obtained by: **a**) direct or indirect (either via organic redox mediators: Med or via hydrogen) electron transfer between the electrode and autotrophic electro-active diazotrophs; **b**) syntrophic interaction (facultatively via direct interspecies electron transfer, DIET) between autotrophs and electroactive diazotrophs; **c**) CH_4-short-circuiting syntrophic interaction between electro-active autotrophs (methanogens) and methanotrophic diazotrophs (furnishing fixed-N to the community); **d**) heterotrophic diazotrophs, harvesting energy from residual organic matter in the biofilm.

References

[1] R. Navarro-Gonzalez, C.P. McKay, D.N. Mvondo, A possible nitrogen crisis for Archaean life due to reduced nitrogen fixation by lightning., Nature. 412 (2001) 61–64. doi:10.1038/35083537.

[2] D. Fowler, M. Coyle, U. Skiba, M.A. Sutton, J.N. Cape, S. Reis, L.J. Sheppard, A. Jenkins, B. Grizzetti, J.N. Galloway, P. Vitousek, A. Leach, A.F. Bouwman, K. Butterbach-Bahl, F. Dentener, D. Stevenson, M. Amann, M. Voss, The global nitrogen cycle in the twenty-first century., Philos. Trans. R. Soc. Lond. B. Biol. Sci. 368 (2013). doi:10.1098/rstb.2013.0164.

[3] K.C. Cameron, H.J. Di, J.L. Moir, Nitrogen losses from the soil/plant system: a review, Ann. Appl. Biol. 162 (2013) 145–173. doi:10.1111/aab.12014.

[4] D.L. Jones, P. Cross, P.J.A. Withers, T.H. DeLuca, D.A. Robinson, R.S. Quilliam, I.M. Harris, D.R. Chadwick, G. Edwards-Jones, REVIEW: Nutrient stripping: the global disparity between food security and soil nutrient stocks, J. Appl. Ecol. 50 (2013) 851–862. doi:10.1111/1365-2664.12089.

[5] F. Mapelli, R. Marasco, M. Fusi, B. Scaglia, G. Tsiamis, E. Rolli, S. Fodelianakis, K. Bourtzis, S. Ventura, F. Tambone, F. Adani, S. Borin, D. Daffonchio, The stage of soil development modulates rhizosphere effect along a High Arctic desert chronosequence, ISME J. (2018). doi:10.1038/s41396-017-0026-4.

[6] F. Adani, G. Papa, F. Tambone, Dynamics and fate of natural and waste organic material in soils : the role of the soil organic matter (SOM) recalcitrance in SOM turnover, 2010 19th World Congr. Soil Sci. (2010) 73–75.

[7] L.S. Hartmann, S.R. Barnum, Inferring the evolutionary history of mo-dependent nitrogen fixation from phylogenetic studies of nifk and nifdk, J. Mol. Evol. 71 (2010) 70–85. doi:10.1007/s00239-010-9365-8.

[8] C. Kneip, P. Lockhart, C. Voß, U.-G. Maier, Nitrogen fixation in eukaryotes – New models for symbiosis, BMC Evol. Biol. 7 (2007) 55. doi:10.1186/1471-2148-7-55.

[9] H. Burgmann, F. Widmer, W. Von Sigler, J. Zeyer, New Molecular Screening Tools for Analysis of Free-Living Diazotrophs in Soil, Appl. Environ. Microbiol. 70 (2004) 240–247. doi:10.1128/AEM.70.1.240-247.2004.

[10] T. Fenchel, G.M. King, T.H. Blackburn, Bacterial Biogeochemistry: the Ecophysiology of Mineral Cycling, 2012. doi:10.1016/B978-0-12-415836-8.00012-8.

[11] X. Wu, K. Pedersen, J. Edlund, L. Eriksson, M. Åström, A.F. Andersson, S. Bertilsson, M. Dopson, Potential for hydrogen-oxidizing chemolithoautotrophic and diazotrophic populations to initiate biofilm formation in oligotrophic, deep terrestrial subsurface waters, Microbiome. 5 (2017) 37. doi:10.1186/s40168-017-0253-y.

[12] L. Duc, M. Noll, B.E. Meier, H. Bürgmann, J. Zeyer, High diversity of diazotrophs in the forefield of a receding alpine glacier, Microb. Ecol. 57 (2009) 179–190. doi:10.1007/s00248-008-9408-5.

[13] G. Reguera, K.D. McCarthy, T. Mehta, J.S. Nicoll, M.T. Tuominen, D.R. Lovley, Extracellular electron transfer via microbial nanowires., Nature. 435 (2005) 1098–101. doi:10.1038/nature03661.

[14] D.E. Holmes, D.R. Bond, R. a. O'Neil, C.E. Reimers, L.R. Tender, D.R. Lovley, Microbial communities associated with electrodes harvesting electricity from a variety of aquatic sediments, Microb. Ecol. 48 (2004) 178–190. doi:10.1007/s00248-003-0004-4.

[15] L. Shi, H. Dong, G. Reguera, H. Beyenal, A. Lu, J. Liu, H.-Q. Yu, J.K. Fredrickson, Extracellular electron transfer mechanisms between microorganisms and minerals, Nat. Rev. Microbiol. (2016). doi:10.1038/nrmicro.2016.93.

[16] J. Valdés, I. Pedroso, R. Quatrini, R.J. Dodson, H. Tettelin, R. Blake, J. a Eisen, D.S. Holmes, Acidithiobacillus ferrooxidans metabolism: from genome sequence to industrial applications., BMC Genomics. 9 (2008) 597. doi:10.1186/1471-2164-9-597.

[17] S. Cheng, D. Xing, D.F. Call, B.E. Logan, Direct Biological Conversion of Electrical Current

into Methane by Electromethanogenesis, Environ. Sci. Technol. 43 (2009) 3953–3958. doi:10.1021/es803531g.

[18] O. Choi, B.-I. Sang, Extracellular electron transfer from cathode to microbes: application for biofuel production, Biotechnol. Biofuels. 9 (2016) 11. doi:10.1186/s13068-016-0426-0.

[19] K.P. Nevin, T.L. Woodard, A.E. Franks, Microbial Electrosynthesis : Feeding Microbial Electrosynthesis : Feeding Microbes Electricity To Convert Carbon Dioxide and Water to Multicarbon Extracellular Organic, Am. Soc. Microbiol. 1 (2010) 1–4. doi:10.1128/mBio.00103-10.Editor.

[20] F. Kracke, J.O. Krömer, Identifying target processes for microbial electrosynthesis by elementary mode analysis, BMC Bioinformatics. 15 (2014) 410–423. doi:10.1186/s12859-014-0410-2.

[21] K. Rabaey, R. a Rozendal, Microbial electrosynthesis - revisiting the electrical route for microbial production., Nat. Rev. Microbiol. 8 (2010) 706–716. doi:10.1038/nrmicro2422.

[22] S. Bajracharya, S. Srikanth, G. Mohanakrishna, R. Zacharia, D.P. Strik, D. Pant, Biotransformation of carbon dioxide in bioelectrochemical systems: State of the art and future prospects, J. Power Sources. 356 (2017) 256–273. doi:10.1016/J.JPOWSOUR.2017.04.024.

[23] F. Kracke, I. Vassilev, J.O. Krömer, Microbial electron transport and energy conservation - the foundation for optimizing bioelectrochemical systems., Front. Microbiol. 6 (2015) 575. doi:10.3389/fmicb.2015.00575.

[24] S. Bajracharya, K. Vanbroekhoven, C.J.N. Buisman, D.P.B.T.B. Strik, D. Pant, Bioelectrochemical conversion of CO_2 to chemicals: CO_2 as a next generation feedstock for electricity-driven bioproduction in batch and continuous modes, Faraday Discuss. 202 (2017) 433–449. doi:10.1039/C7FD00050B.

[25] B.J. Eddie, Z. Wang, W.J. Hervey, D.H. Leary, A.P. Malanoski, L.M. Tender, B. Lin, S.M. Strycharz-Glaven, Metatranscriptomics Supports the Mechanism for Biocathode Electroautotrophy by " *Candidatus* Tenderia electrophaga," MSystems. 2 (2017) e00002-17. doi:10.1128/mSystems.00002-17.

[26] C.W. Marshall, D.E. Ross, E.B. Fichot, R.S. Norman, H.D. May, Long-term operation of microbial electrosynthesis systems improves acetate production by autotrophic microbiomes, Environ. Sci. Technol. 47 (2013) 6023–6029. doi:10.1021/es400341b.

[27] A. Schievano, T. Pepé Sciarria, K. Vanbroekhoven, H. De Wever, S. Puig, S.J. Andersen, K. Rabaey, D. Pant, Electro-Fermentation – Merging Electrochemistry with Fermentation in Industrial Applications, Trends Biotechnol. 34 (2016) 866–878. doi:10.1016/j.tibtech.2016.04.007.

[28] S. Bajracharya, A. ter Heijne, X.D. Benetton, K. Vanbroekhoven, C.J.N. Buisman, D.P.B.T.B. Strik, D. Pant, Carbon dioxide reduction by mixed and pure cultures in microbial electrosynthesis using an assembly of graphite felt and stainless steel as a cathode, Bioresour. Technol. 195 (2015) 14–24. doi:10.1016/j.biortech.2015.05.081.

[29] D.E. Holmes, P.M. Shrestha, D.J.F. Walker, Y. Dang, K.P. Nevin, T.L. Woodard, D.R. Lovley, Metatranscriptomic evidence for direct interspecies electron transfer between Geobacter and Methanothrix species in methanogenic rice paddy soils, Appl. Environ. Microbiol. 83 (2017) AEM.00223-17. doi:10.1128/AEM.00223-17.

[30] R.D. Milton, R. Cai, S. Sahin, S. Abdellaoui, B. Alkotaini, D. Leech, S.D. Minteer, The in Vivo Potential-Regulated Protective Protein of Nitrogenase in Azotobacter vinelandii Supports Aerobic Bioelectrochemical Dinitrogen Reduction in Vitro, J. Am. Chem. Soc. 139 (2017) 9044–9052. doi:10.1021/jacs.7b04893.

[31] T.M. Paschkewitz, Ammonia Production at Ambient Temperature and Pressure : An Electrochemical and Biological Approach, (2012).

[32] J. Leddy, T.M. Paschkewitz, Ammonia production using bioelectrocatalytical devices, US 2014/0011252 A1, 2014.

[33] C. Liu, K.K. Sakimoto, B.C. Colón, P.A. Silver, D.G. Nocera, Ambient nitrogen reduction cycle using a hybrid inorganic–biological system, Proc. Natl. Acad. Sci. 114 (2017) 6450–6455. doi:10.1073/pnas.1706371114.

[34] S. Kalathil, D. Pant, Nanotechnology to rescue bacterial bidirectional extracellular electron transfer in bioelectrochemical systems, RSC Adv. 6 (2016) 30582–30597. doi:10.1039/C6RA04734C.

[35] J.R. Andreesen, G. Gottschalk, H.G. Schlegel, Clostridium formicoaceticum nov. spec. Isolation, description and distinction from C. aceticum and C. thermoaceticum, Arch. Mikrobiol. 72 (1970) 154–174. doi:10.1007/BF00409521.

[36] L.G. Rebits, D.J. Bennett, P.A. Bhagwat, A. Morin, R.E. Sievers, Method for quantifying the sample collected by an Andersen Cascade Impactor using total organic carbon analysis, J. Aerosol Sci. 38 (2007) 1197–1206. doi:10.1016/j.jaerosci.2007.09.005.

[37] S. Zecchin, A. Corsini, M. Martin, M. Romani, G.M. Beone, R. Zanchi, E. Zanzo, D. Tenni, M.C. Fontanella, L. Cavalca, Rhizospheric iron and arsenic bacteria affected by water regime: Implications for metalloid uptake by rice, Soil Biol. Biochem. 106 (2017) 129–137. doi:10.1016/j.soilbio.2016.12.021.

[38] A. Schievano, A. Tenca, S. Lonati, E. Manzini, F. Adani, Can two-stage instead of one-stage anaerobic digestion really increase energy recovery from biomass?, Appl. Energy. 124 (2014) 335–342.

[39] F. Villa, W. Remelli, F. Forlani, M. Gambino, P. Landini, F. Cappitelli, Effects of chronic sub-lethal oxidative stress on biofilm formation by Azotobacter vinelandii, Biofouling. 28 (2012) 823–833. doi:10.1080/08927014.2012.715285.

[40] F. Villa, B. Pitts, E. Lauchnor, F. Cappitelli, P.S. Stewart, Development of a Laboratory Model of a Phototroph-Heterotroph Mixed-Species Biofilm at the Stone/Air Interface, Front. Microbiol. 6 (2015). doi:10.3389/fmicb.2015.01251.

[41] S. Nurk, A. Bankevich, D. Antipov, A.A. Gurevich, A. Korobeynikov, A. Lapidus, A.D. Prjibelski, A. Pyshkin, A. Sirotkin, Y. Sirotkin, R. Stepanauskas, S.R. Clingenpeel, T. Woyke, J.S. Mclean, R. Lasken, G. Tesler, M.A. Alekseyev, P.A. Pevzner, Assembling Single-Cell Genomes and Mini-Metagenomes From Chimeric MDA Products, J. Comput. Biol. 20 (2013) 714–737. doi:10.1089/cmb.2013.0084.

[42] D.A. Antonopoulos, E.M. Glass, F. Meyer, Analyzing Metagenomic Data: Inferring Microbial Community Function with MG-RAST, in: Metagenomics Its Appl. Agric. Biomed. Environ. Stud., Agricultural Research Service, 2010: pp. 47–60.

[43] R. Tatusow, M. Galperin, D. Natale, E. Koonin, The COG database: a tool for genome-scale analysis of protein functions and evolution, Nucleic Acids Res. 28 (2000) 33–36.

[44] M. Johnson, I. Zaretskaya, Y. Raytselis, Y. Merezhuk, S. McGinnis, T.L. Madden, NCBI BLAST: a better web interface, Nucleic Acids Res. 36 (2008) W5–W9. doi:10.1093/nar/gkn201.

[45] K. Tamura, G. Stecher, D. Peterson, A. Filipski, S. Kumar, MEGA6: Molecular Evolutionary Genetics Analysis Version 6.0, Mol. Biol. Evol. 30 (2013) 2725–2729. doi:10.1093/molbev/mst197.

[46] K. Stoecker, C. Dorninger, H. Daims, M. Wagner, Double Labeling of Oligonucleotide Probes for Fluorescence In Situ Hybridization (DOPE-FISH) Improves Signal Intensity and Increases rRNA Accessibility, Appl. Environ. Microbiol. 76 (2010) 922–926. doi:10.1128/AEM.02456-09.

[47] F. Cappitelli, F. Villa, A. Polo, Culture-Independent Methods to Study Subaerial Biofilm Growing on Biodeteriorated Surfaces of Stone Cultural Heritage and Frescoes, in: 2014: pp. 341–366. doi:10.1007/978-1-4939-0467-9_24.

[48] F. Villa, F. Cappitelli, P. Principi, A. Polo, C. Sorlini, Permeabilization method for in-situ investigation of fungal conidia on surfaces, Lett. Appl. Microbiol. 48 (2009) 234–240. doi:10.1111/j.1472-765X.2008.02520.x.

[49] N. Fierer, J.A. Jackson, R. Vilgalys, R.B. Jackson, Assessment of soil microbial community structure by use of taxon-specific quantitative PCR assays., Appl. Environ. Microbiol. 71 (2005) 4117–20. doi:10.1128/AEM.71.7.4117-4120.2005.

[50] Y. Yu, C. Lee, J. Kim, S. Hwang, Group-specific primer and probe sets to detect methanogenic communities using quantitative real-time polymerase chain reaction, Biotechnol. Bioeng. 89 (2005) 670–679. doi:10.1002/bit.20347.

[51] L. Rago, Y. Ruiz, J.A. Baeza, A. Guisasola, P. Cortés, Microbial community analysis in a long-term membrane-less microbial electrolysis cell with hydrogen and methane production, Bioelectrochemistry. 106 (2015) 359–368. doi:10.1016/j.bioelechem.2015.06.003.

[52] S.J. Green, R. Venkatramanan, A. Naqib, Deconstructing the Polymerase Chain Reaction: Understanding and Correcting Bias Associated with Primer Degeneracies and Primer-Template Mismatches, PLoS One. 10 (2015) e0128122. doi:10.1371/journal.pone.0128122.

[53] S.M. Bybee, H. Bracken-Grissom, B.D. Haynes, R.A. Hermansen, R.L. Byers, M.J. Clement, J.A. Udall, E.R. Wilcox, K.A. Crandall, Targeted Amplicon Sequencing (TAS): A Scalable Next-Gen Approach to Multilocus, Multitaxa Phylogenetics, Genome Biol. Evol. 3 (2011) 1312–1323. doi:10.1093/gbe/evr106.

[54] L. Rago, P. Cristiani, F. Villa, S. Zecchin, A. Colombo, L. Cavalca, A. Schievano, Influences of dissolved oxygen concentration on biocathodic microbial communities in microbial fuel cells, Bioelectrochemistry. 116 (2017) 39–51. doi:10.1016/j.bioelechem.2017.04.001.

[55] P. V. Moonsamy, T. Williams, P. Bonella, C.L. Holcomb, B.N. Höglund, G. Hillman, D. Goodridge, G.S. Turenchalk, L.A. Blake, D.A. Daigle, B.B. Simen, A. Hamilton, A.P. May, H.A. Erlich, High throughput HLA genotyping using 454 sequencing and the Fluidigm Access Array™ system for simplified amplicon library preparation, Tissue Antigens. 81 (2013) 141–149. doi:10.1111/tan.12071.

[56] J. Zhang, K. Kobert, T. Flouri, A. Stamatakis, PEAR: a fast and accurate Illumina Paired-End reAd mergeR, Bioinformatics. 30 (2014) 614–620. doi:10.1093/bioinformatics/btt593.

[57] R.C. Edgar, Search and clustering orders of magnitude faster than BLAST, Bioinformatics. 26 (2010) 2460–2461. doi:10.1093/bioinformatics/btq461.

[58] J.G. Caporaso, J. Kuczynski, J. Stombaugh, K. Bittinger, F.D. Bushman, E.K. Costello, N. Fierer, A.G. Peña, J.K. Goodrich, J.I. Gordon, G.A. Huttley, S.T. Kelley, D. Knights, J.E. Koenig, R.E. Ley, C.A. Lozupone, D. McDonald, B.D. Muegge, M. Pirrung, J. Reeder, J.R. Sevinsky, P.J. Turnbaugh, W.A. Walters, J. Widmann, T. Yatsunenko, J. Zaneveld, R. Knight, QIIME allows analysis of high-throughput community sequencing data, Nat. Methods. 7 (2010) 335–336. doi:10.1038/nmeth.f.303.

[59] C. Quast, E. Pruesse, P. Yilmaz, J. Gerken, T. Schweer, P. Yarza, J. Peplies, F.O. Glockner, The SILVA ribosomal RNA gene database project: improved data processing and web-based tools, Nucleic Acids Res. 41 (2013) D590–D596. doi:10.1093/nar/gks1219.

[60] J.G. Caporaso, K. Bittinger, F.D. Bushman, T.Z. DeSantis, G.L. Andersen, R. Knight, PyNAST: a flexible tool for aligning sequences to a template alignment, Bioinformatics. 26 (2010) 266–267. doi:10.1093/bioinformatics/btp636.

[61] C.M. Paquete, B.M. Fonseca, D.R. Cruz, T.M. Pereira, I. Pacheco, C.M. Soares, R.O. Louro, Exploring the molecular mechanisms of electron shuttling across the microbe/metal space, Front. Microbiol. 5 (2014) 318. doi:10.3389/fmicb.2014.00318.

[62] S.E. Neto, D. de Melo-Diogo, I.J. Correia, C.M. Paquete, R.O. Louro, Characterization of OmcA Mutants from *Shewanella oneidensis* MR-1 to Investigate the Molecular Mechanisms Underpinning Electron Transfer Across the Microbe-Electrode Interface, Fuel Cells. 17 (2017) 601–611. doi:10.1002/fuce.201700023.

[63] T. Hurek, B. Reinhold-Hurek, Azoarcus sp. strain BH72 as a model for nitrogen-fixing grass endophytes, J. Biotechnol. 106 (2003) 169–178. doi:10.1016/J.JBIOTEC.2003.07.010.

[64] J.-H. Chou, S.-R. Jiang, J.-C. Cho, J. Song, M.-C. Lin, W.-M. Chen, Azonexus hydrophilus sp. nov., a nifH gene-harbouring bacterium isolated from freshwater, Int. J. Syst. Evol.

Microbiol. 58 (2008) 946–951. doi:10.1099/ijs.0.65434-0.
[65] J.M. Macy, S. Rech, G. Auling, M. Dorsch, E. Stackebrandt, L.I. Sly, Thauera selenatis gen. nov., sp. nov., a Member of the Beta Subclass of Proteobacteria with a Novel Type of Anaerobic Respiration, Int. J. Syst. Bacteriol. 43 (1993) 135–142. doi:10.1099/00207713-43-1-135.
[66] B. Liu, F. Zhang, X. Feng, Y. Liu, X. Yan, X. Zhang, L. Wang, L. Zhao, Thauera and Azoarcus as functionally important genera in a denitrifying quinoline-removal bioreactor as revealed by microbial community structure comparison, FEMS Microbiol. Ecol. 55 (2006) 274–286. doi:10.1111/j.1574-6941.2005.00033.x.
[67] T. Ogiso, C. Ueno, D. Dianou, T. Van Huy, A. Katayama, M. Kimura, S. Asakawa, Methylomonas koyamae sp. nov., a type I methane-oxidizing bacterium from floodwater of a rice paddy field, Int. J. Syst. Evol. Microbiol. 62 (2012) 1832–1837. doi:10.1099/ijs.0.035261-0.
[68] S. Hoefman, D. van der Ha, N. Boon, P. Vandamme, P. De Vos, K. Heylen, Niche differentiation in nitrogen metabolism among methanotrophs within an operational taxonomic unit, BMC Microbiol. 14 (2014) 83. doi:10.1186/1471-2180-14-83.
[69] A.J.M. Stams, C.M. Plugge, Electron transfer in syntrophic communities of anaerobic bacteria and archaea, Nat. Rev. Microbiol. 7 (2009) 568–77. https://search.proquest.com/openview/47677751cf67fed92e6e35967b734e38/1?pq-origsite=gscholar&cbl=27584 (accessed July 23, 2017).
[70] S. Asakawa, H. Morii, M. Akagawa-Matsushita, Y. Koga, K. Hayano, Characterization of Methanobrevibacter arboriphilicus SA Isolated from a Paddy Field Soil and DNA-DNA Hybridization among M. arboriphilicus strains, Int. J. Syst. Bacteriol. 44 (1994) 185–185. doi:10.1099/00207713-44-1-185.
[71] Y. Jiang, M. Su, D. Li, Removal of Sulfide and Production of Methane from Carbon Dioxide in Microbial Fuel Cells–Microbial Electrolysis Cell (MFCs–MEC) Coupled System, Appl. Biochem. Biotechnol. 172 (2014) 2720–2731. doi:10.1007/s12010-013-0718-9.
[72] M. Zeppilli, M. Villano, F. Aulenta, S. Lampis, G. Vallini, M. Majone, Effect of the anode feeding composition on the performance of a continuous-flow methane-producing microbial electrolysis cell, Environ. Sci. Pollut. Res. 22 (2015) 7349–7360. doi:10.1007/s11356-014-3158-3.
[73] L. Shen, Q. Zhao, X. Wu, X. Li, Q. Li, Y. Wang, Interspecies electron transfer in syntrophic methanogenic consortia: From cultures to bioreactors, Renew. Sustain. Energy Rev. 54 (2016) 1358–1367. doi:10.1016/J.RSER.2015.10.102.
[74] S. Pirbadian, S.E. Barchinger, K.M. Leung, H.S. Byun, Y. Jangir, R.A. Bouhenni, S.B. Reed, M.F. Romine, D.A. Saffarini, L. Shi, Y.A. Gorby, J.H. Golbeck, M.Y. El-Naggar, Shewanella oneidensis MR-1 nanowires are outer membrane and periplasmic extensions of the extracellular electron transport components, Proc. Natl. Acad. Sci. 111 (2014) 12883–12888. doi:10.1073/pnas.1410551111.
[75] H.G. Martin, N. Ivanova, V. Kunin, F. Warnecke, K.W. Barry, A.C. McHardy, C. Yeates, S. He, A.A. Salamov, E. Szeto, E. Dalin, N.H. Putnam, H.J. Shapiro, J.L. Pangilinan, I. Rigoutsos, N.C. Kyrpides, L.L. Blackall, K.D. McMahon, P. Hugenholtz, Metagenomic analysis of two enhanced biological phosphorus removal (EBPR) sludge communities, Nat Biotech. 24 (2006) 1263–1269. http://dx.doi.org/10.1038/nbt1247.
[76] J. Liu, Z. Wang, S.M. Belchik, M.J. Edwards, C. Liu, D.W. Kennedy, E.D. Merkley, M.S. Lipton, J.N. Butt, D.J. Richardson, J.M. Zachara, J.K. Fredrickson, K.M. Rosso, L. Shi, Identification and Characterization of MtoA: A Decaheme c-Type Cytochrome of the Neutrophilic Fe(II)-Oxidizing Bacterium Sideroxydans lithotrophicus ES-1., Front. Microbiol. 3 (2012) 37. doi:10.3389/fmicb.2012.00037.
[77] S. Kato, S. Krepski, C. Chan, T. Itoh, M. Ohkuma, Ferriphaselus amnicola gen. nov., sp. nov., a neutrophilic, stalk-forming, iron-oxidizing bacterium isolated from an iron-rich

groundwater seep, Int. J. Syst. Evol. Microbiol. 64 (2014) 921–925. doi:10.1099/ijs.0.058487-0.

Highlights:

- We introduce a new type of microbial electrosynthesis: bioelectrochemical N-fixation
- e-BNF aims at producing whole biomass from N_2 and inorganic carbon
- Electrostimulation of microbial communities enriched autotrophic N-fixers
- Biomass synthesis was higher, as compared to open circuit conditions
- e-BNF is a possible candidate for sustainable alternatives to Haber-Bosch process

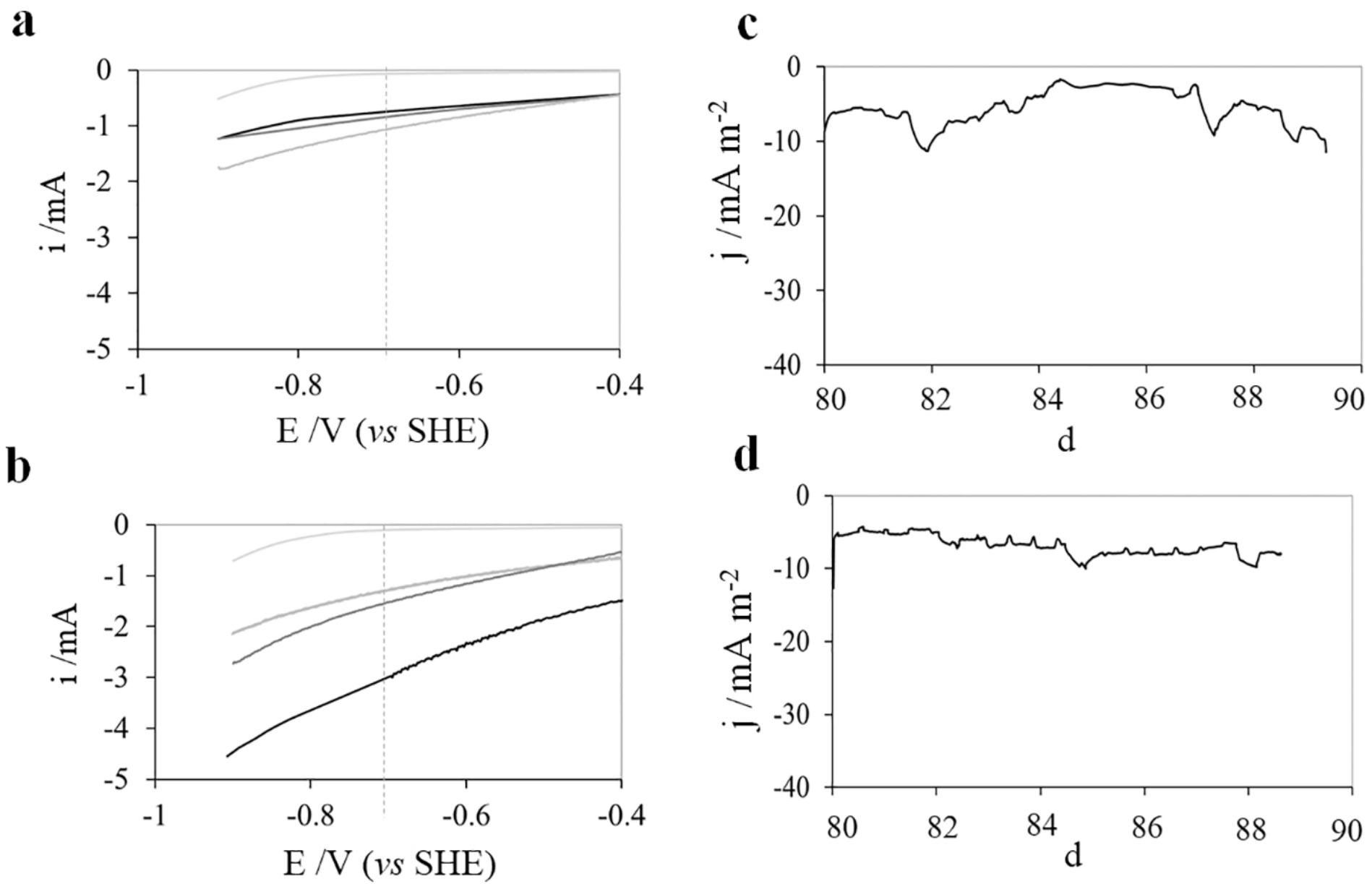
a
0
-1
-2
-3
-4
-5
i /mA
-1
-0.8
-0.6
-0.4
E /V (vs SHE)
b
0
-1
-2
-3
-4
-5
i /mA
-1
-0.8
-0.6
-0.4
E /V (vs SHE)
c
0
-10
-20
-30
-40
j /mA m-2
80
82
84
86
88
90
d
d
0
-10
-20
-30
-40
j / mA m-2
80
82
84
86
88
90
d

Figure 1

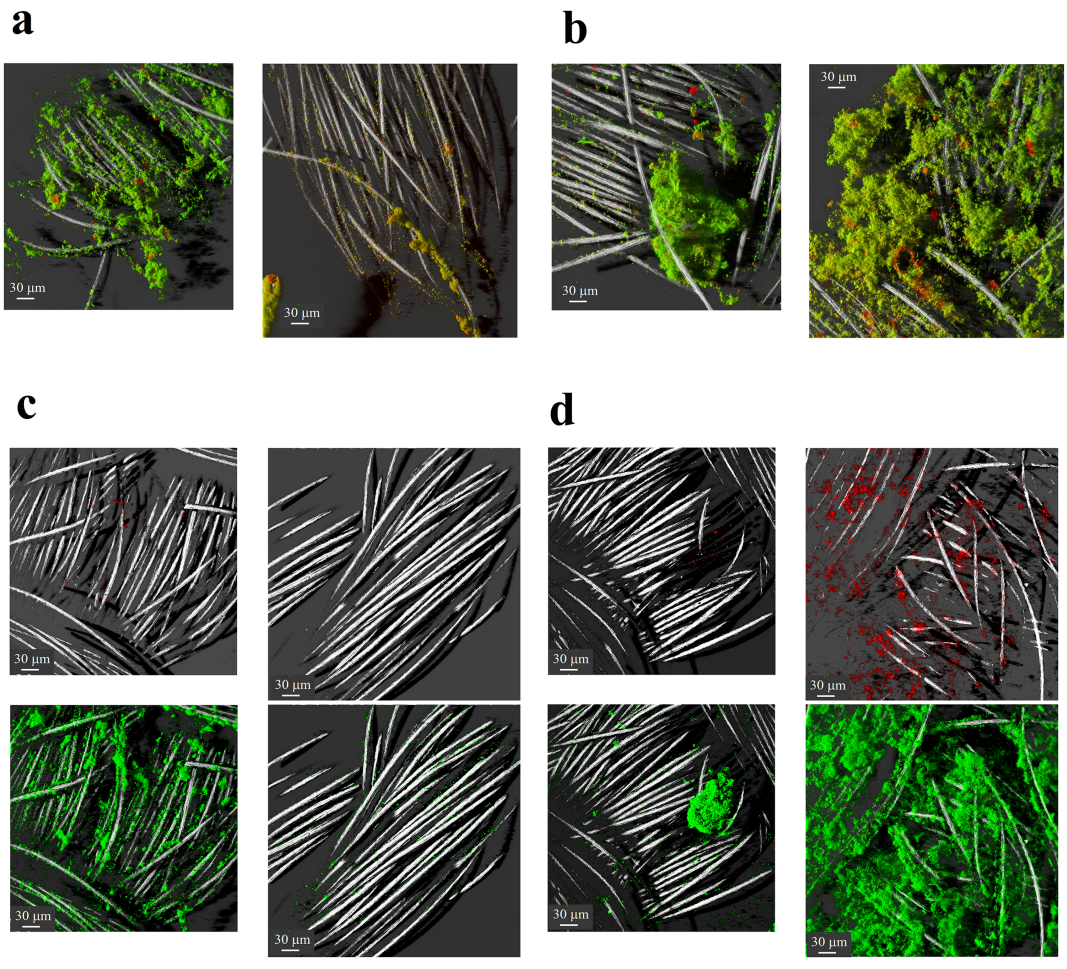

Figure 2

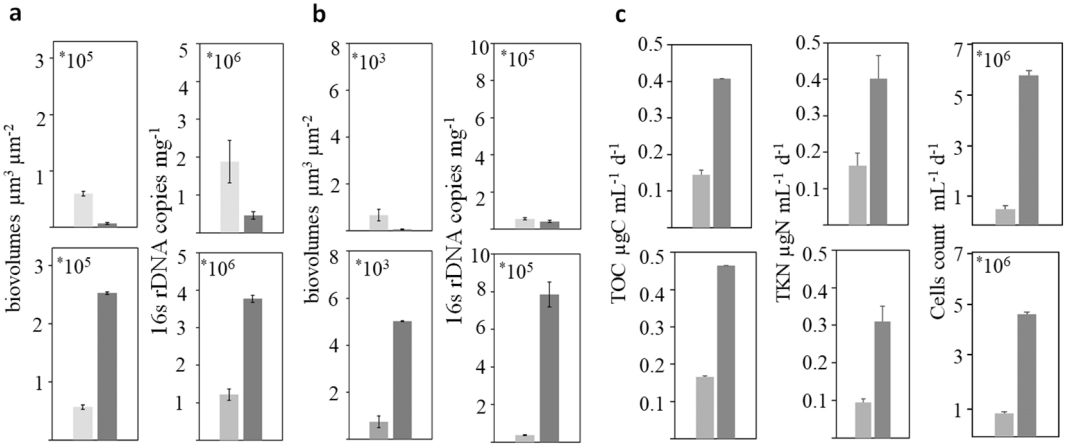
a
b
c
biovolumes µm³ µm⁻²
16s rDNA copies mg⁻¹
TOC µgC mL⁻¹ d⁻¹
TKN µgN mL⁻¹ d⁻¹
Cells count mL⁻¹ d⁻¹
*10⁵
*10⁶
*10³

Figure 3

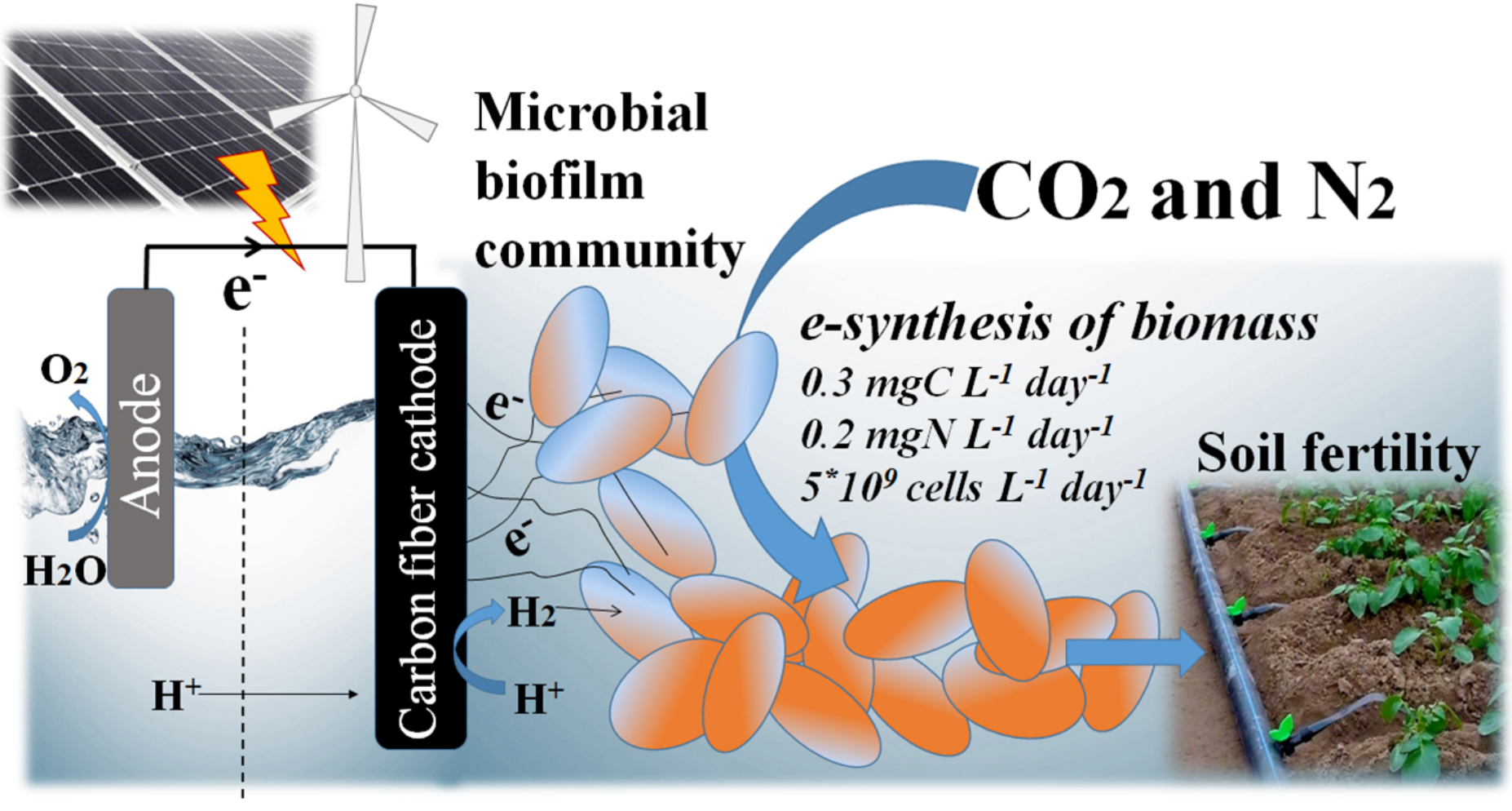
Microbial
biofilm
community
CO2 and N2
e-synthesis of biomass
0.3 mgC L-1 day-1
0.2 mgN L-1 day-1
5*10^9 cells L-1 day-1
Soil fertility
e-
O2
Anode
H2O
Carbon fiber cathode
e-
e-
H2
H+
H+

Figure 4

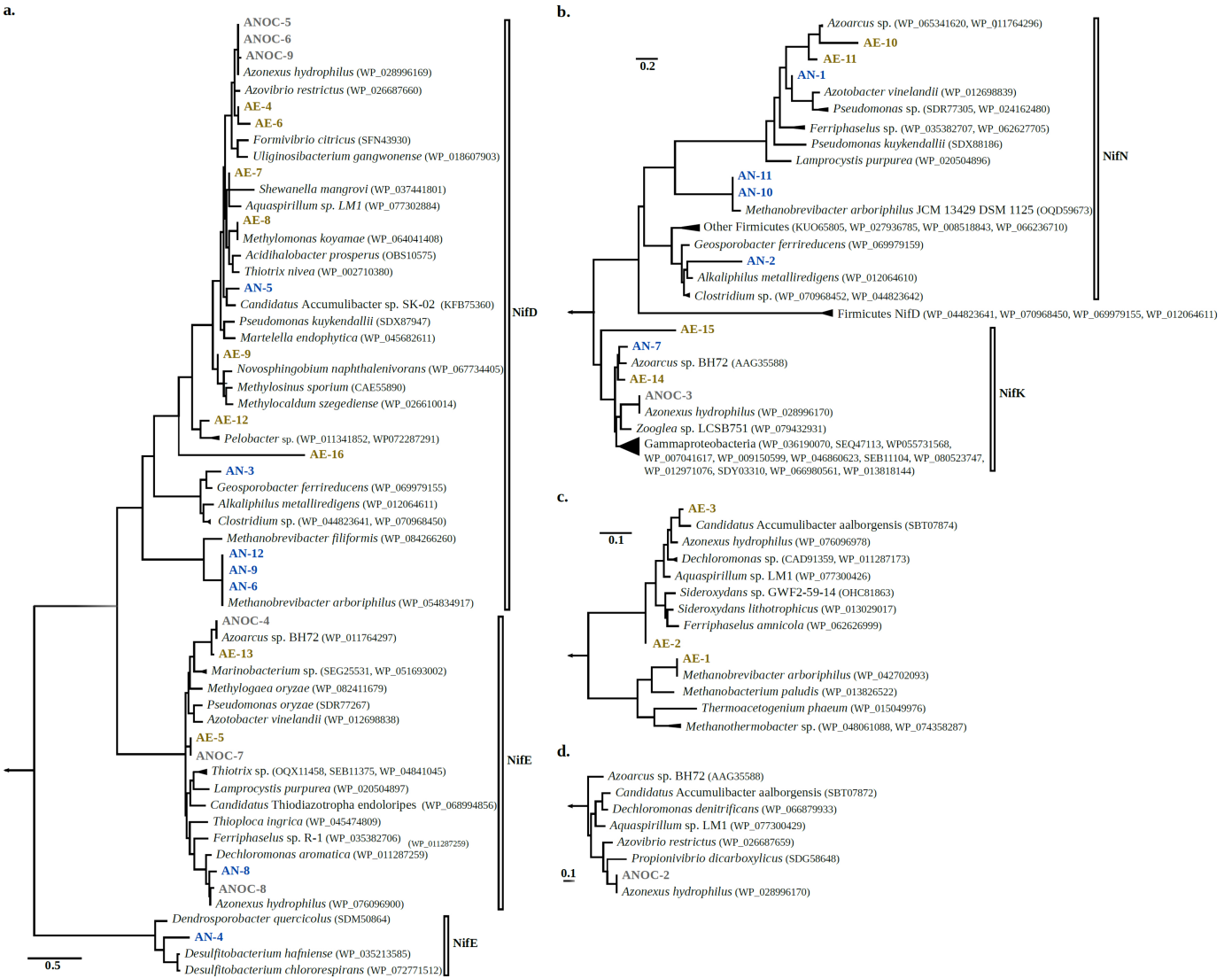
a.
ANOC-5
ANOC-6
ANOC-9
Azonexus hydrophilus (WP_028996169)
Azovibrio restrictus (WP_026687660)
AE-4
AE-6
Formivibrio citricus (SFN43930)
Uliginosibacterium gangwonense (WP_018607903)
AE-7
Shewanella mangrovi (WP_037441801)
Aquaspirillum sp. LM1 (WP_077302884)
AE-8
Methylomonas koyamae (WP_064041408)
Acidihalobacter prosperus (OBS10575)
Thiotrix nivea (WP_002710380)
AN-5
Candidatus Accumulibacter sp. SK-02 (KFB75360)
Pseudomonas kuykendallii (SDX87947)
Martelella endophytica (WP_045682611)
AE-9
Novosphingobium naphthalenivorans (WP_067734405)
Methylosinus sporium (CAE55890)
Methylocaldum szegediense (WP_026610014)
AE-12
Pelobacter sp. (WP_011341852, WP072287291)
AE-16
NifD
AN-3
Geosporobacter ferrireducens (WP_069979155)
Alkaliphilus metalliredigens (WP_012064611)
Clostridium sp. (WP_044823641, WP_070968450)
Methanobrevibacter filiformis (WP_084266260)
AN-12
AN-9
AN-6
Methanobrevibacter arboriphilus (WP_054834917)
ANOC-4
Azoarcus sp. BH72 (WP_011764297)
AE-13
Marinobacterium sp. (SEG25531, WP_051693002)
Methylogaea oryzae (WP_082411679)
Pseudomonas oryzae (SDR77267)
Azotobacter vinelandii (WP_012698838)
AE-5
ANOC-7
Thiotrix sp. (OQX11458, SEB11375, WP_04841045)
Lamprocystis purpurea (WP_020504897)
Candidatus Thiodiazotropha endoloripes (WP_068994856)
Thioploca ingrica (WP_045474809)
Ferriphaselus sp. R-1 (WP_035382706) (WP_011287259)
Dechloromonas aromatica (WP_011287259)
AN-8
ANOC-8
Azonexus hydrophilus (WP_076096900)
NifE
Dendrosporobacter quercicolus (SDM50864)
AN-4
Desulfitobacterium hafniense (WP_035213585)
Desulfitobacterium chlororespirans (WP_072771512)
NifE
0.5
b.
0.2
Azoarcus sp. (WP_065341620, WP_011764296)
AE-10
AE-11
AN-1
Azotobacter vinelandii (WP_012698839)
Pseudomonas sp. (SDR77305, WP_024162480)
Ferriphaselus sp. (WP_035382707, WP_062627705)
Pseudomonas kuykendallii (SDX88186)
Lamprocystis purpurea (WP_020504896)
NifN
AN-11
AN-10
Methanobrevibacter arboriphilus JCM 13429 DSM 1125 (OQD59673)
Other Firmicutes (KUO65805, WP_027936785, WP_008518843, WP_066236710)
Geosporobacter ferrireducens (WP_069979159)
AN-2
Alkaliphilus metalliredigens (WP_012064610)
Clostridium sp. (WP_070968452, WP_044823642)
Firmicutes NifD (WP_044823641, WP_070968450, WP_069979155, WP_012064611)
AE-15
AN-7
Azoarcus sp. BH72 (AAG35588)
AE-14
ANOC-3
Azonexus hydrophilus (WP_028996170)
Zooglea sp. LCSB751 (WP_079432931)
Gammaproteobacteria (WP_036190070, SEQ47113, WP055731568, WP_007041617, WP_009150599, WP_046860623, SEB11104, WP_080523747, WP_012971076, SDY03310, WP_066980561, WP_013818144)
NifK
c.
0.1
AE-3
Candidatus Accumulibacter aalborgensis (SBT07874)
Azonexus hydrophilus (WP_076096978)
Dechloromonas sp. (CAD91359, WP_011287173)
Aquaspirillum sp. LM1 (WP_077300426)
Sideroxydans sp. GWF2-59-14 (OHC81863)
Sideroxydans lithotrophicus (WP_013029017)
Ferriphaselus amnicola (WP_062626999)
AE-2
AE-1
Methanobrevibacter arboriphilus (WP_042702093)
Methanobacterium paludis (WP_013826522)
Thermoacetogenium phaeum (WP_015049976)
Methanothermobacter sp. (WP_048061088, WP_074358287)
d.
Azoarcus sp. BH72 (AAG35588)
Candidatus Accumulibacter aalborgensis (SBT07872)
Dechloromonas denitrificans (WP_066879933)
Aquaspirillum sp. LM1 (WP_077300429)
Azovibrio restrictus (WP_026687659)
Propionivibrio dicarboxylicus (SDG58648)
0.1
ANOC-2
Azonexus hydrophilus (WP_028996170)

Figure 5

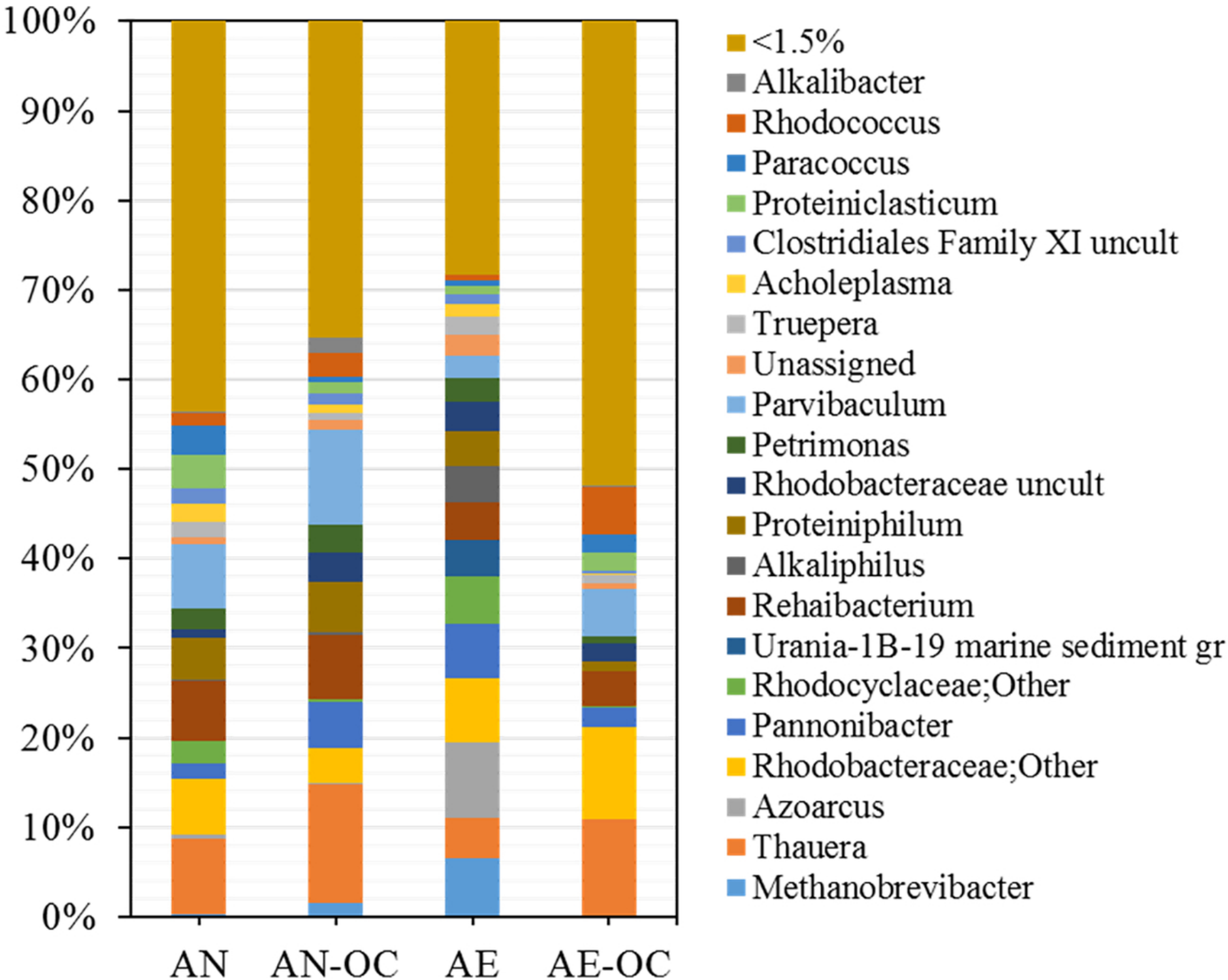
100%
90%
80%
70%
60%
50%
40%
30%
20%
10%
0%
AN
AN-OC
AE
AE-OC
<1.5%
Alkalibacter
Rhodococcus
Paracoccus
Proteiniclasticum
Clostridiales Family XI uncult
Acholeplasma
Truepera
Unassigned
Parvibaculum
Petrimonas
Rhodobacteraceae uncult
Proteiniphilum
Alkaliphilus
Rehaibacterium
Urania-1B-19 marine sediment gr
Rhodocyclaceae;Other
Pannonibacter
Rhodobacteraceae;Other
Azoarcus
Thauera
Methanobrevibacter

Figure 6

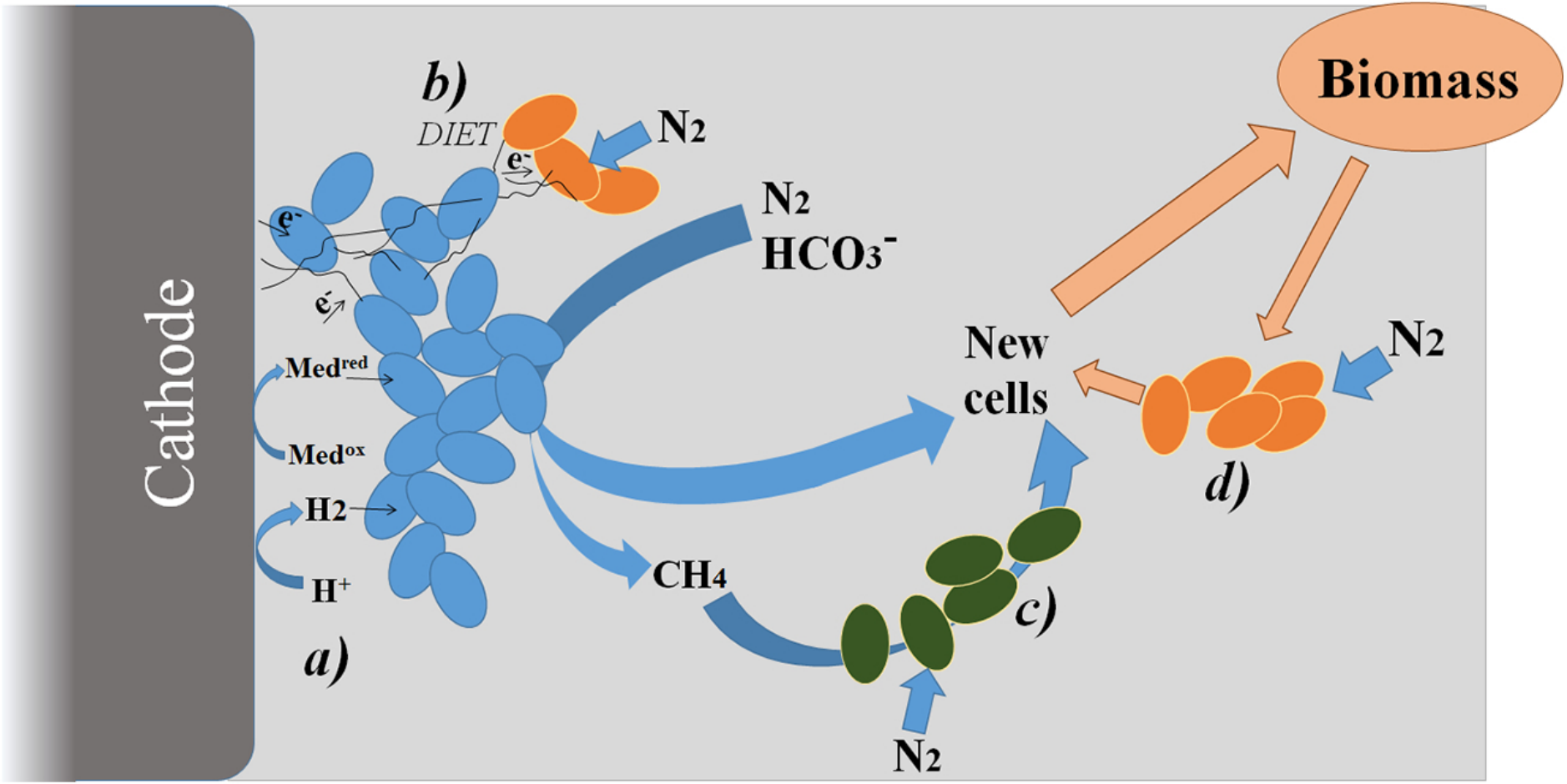
Cathode
b)
DIET
e-
N2
e-
e-
N2
HCO3-
Biomass
New
cells
N2
Med red
Med ox
H2
H+
a)
CH4
c)
d)
N2

Figure 7